JETIR.ORG

# ISSN: 2349-5162 | ESTD Year : 2014 | Monthly Issue JOURNAL OF EMERGING TECHNOLOGIES AND



# INNOVATIVE RESEARCH (JETIR)

An International Scholarly Open Access, Peer-reviewed, Refereed Journal

# BaTiO<sub>3</sub> BASED FERROELECTRICS: HISTORY, CURRENT STATUS, PERSPECTIVES

<sup>1</sup>Salunkhe S. R., <sup>2</sup>Patil S. A., <sup>3</sup>Jadhav L. D.

<sup>1</sup>Research Student, <sup>2</sup>Assistant Professor, <sup>3</sup>Professor <sup>1</sup>Department of physics <sup>1</sup>Government College of engineering Karad 415124, India.

Abstract: we present a critical review of lead-free barium titanate-based piezo-electrics. Ferroelectric materials refer to the group of dielectrics that holds spontaneous polarization. Lead-free BaTiO<sub>3</sub> (Barium Titanate) plays a very important role in industrial areas because of its different type of applications due to its better ferroelectric properties and large dielectrics constant. Barium titanate is better ferroelectric material and its structural, dielectric, and electric properties can be alternated by replacing dopants or ions In this review paper BaTiO<sub>3</sub>-based ferroelectric materials were deliberated, and recapped the resolution of different studies by changing various synthesis methods such as spray pyrolysis, solution growth technique, solid state reaction method, mixed oxide technique, sol gel method, magnetron sputtering, and ceramic method and so on. And ranging shape of nanomaterial's. By replacing dopant like Ca, Zr, Fe and La etc. because of doping in BaTiO<sub>3</sub>, materials achieve good electrical and dielectric properties compared to pure BaTiO<sub>3</sub> these properties observed, velocity of the longitudinal ultrasonic waves (V<sub>L</sub>= 5980.9 m/s), velocity of transverse ultrasonic waves ( $V_T = 3550.6 \text{ m/s}$ ), Young's modulus(E = 163.88 GPa) and the shear modulus (G = 66.73 GPa) Then by changing sintering temperature such as 1350°C to 1400°C of BZT sample indicates the good values of remnant polarization like 35μC/cm<sup>2</sup> and better dielectric constant like 1700 were observed. BCT-BZT composite it shows the good elastic, mechanical and dielectric properties such as residual stress of 1.66 GPa, remnant polarization value ( $P_r = 10 \,\mu\text{C/cm}^2$ ), coercive field value ( $V_C = 5V$ ), dielectric permittivity is 265 at 1 kHz and the dielectric loss value 0.2. (XRD) X-Ray Diffraction and SEM (Scanning Electron Microscope) indicates the average crystallite size ranging from 40 nm to 80 nm and TG-DTA (Thermogravimetric - Differential Thermal Analysis) is measured total weight loss of about 1.73%. These results will give a brief knowledge of the existing literature on the few literatures published so far in this field.

Keywords - BaTiO<sub>3</sub>, Nanomaterial, XRD, TG - DTA, Dielectric constant, Nanoparticles.

#### 1. History

#### 1.1 Ferroelectric Ceramics

Ceramic materials with better ferroelectric properties have been developed and utilized for a different type of applications. Among these, the perovskite family having a structure of the type ABO<sub>3</sub> is the most famous type in ferroelectric materials. Many ferroelectric ceramics materials such as; Barium Titanate (BaTiO<sub>3</sub>), Lead Zirconate Titanate (PZT), Lead Titanate (PbTiO<sub>3</sub>) and Lead Lanthanum Zirconate Titanate (PLZT) [1,2]. Brief information of all these materials is given in the following.

#### 1.2 (PbTiO<sub>3</sub>, PT) Lead Titanate

Ferroelectric material such as Lead Titanate having a similar structure as BaTiO<sub>3</sub> with a higher Curie point (450°C). The paraelectric to the ferroelectric Phase transition takes place because of decreasing the temperature through the Curie point. Lead titanate ceramics are very very difficult to fabricated in the bulk form because of a larger volume change on cooling below the Curie point that why the original PbTiO<sub>3</sub> crack and fracture during fabrication process [1,2].

# 1.3 {Pb (Zr<sub>x</sub>Ti<sub>1-x</sub>) O<sub>3</sub>, PZT} Lead Zirconate Titanate

Lead zirconate titanate (PZT) is a binary solid solution of these two materials one is PbZrO<sub>3</sub> an ant ferroelectric and second is PbTiO<sub>3</sub> a ferroelectric. A perovskite-type structure of PZT with Ti<sup>4+</sup> and Zr<sup>4+</sup> ions randomly occupying the B site. At high temperature, PZT has a Paraelectric that is cubic perovskite structure. When cooled below the Curie point line, a

phase transition occurs in the structure resulting in the formation of a ferroelectric tetragonal or rhombohedral phase. They can be used for applications requiring very good ferroelectric properties [1,2].

#### 1.4 (PLZT) Lead Lanthanum Zirconate Titanate

PLZT is a ceramic material of transparent ferroelectric created by doping La<sup>3+</sup> ions on the A sites of lead titanium zirconate (PZT). PLZT ceramics have the similar structure (perovskite) as BaTiO<sub>3</sub> and PZT. PLZT has led to use in electro-optical applications because of its transparent nature. The reduction of the anisotropy of the PZT crystal structure by La<sup>3+</sup> substitution and the ability to obtain pore-free ceramics either by hot pressing or liquid phase sintering these two factors that are responsible for obtaining transparent PLZT ceramics. The general formula for PLZT is given by (Pb<sub>1-x</sub>La<sub>x</sub>) (Zr<sub>1-y</sub>Ti<sub>y</sub>)<sub>1-x/4</sub>O<sub>3</sub>VB<sub>0.25x</sub>O<sub>3</sub> and (Pb<sub>1-x</sub>La<sub>x</sub>)<sub>1-0.5x</sub>(Zr<sub>1-y</sub>Ti<sub>y</sub>)VA<sub>0.5x</sub>O<sub>3</sub>. The first formula shows that La<sup>3+</sup> ions go to site A and vacancies (VB) are created at site B to maintain charge balance and the second formula shows that vacancies are created on site A. The combination of vacancies A and B indicates the actual structure of PLZT [1, 2].

## 1.5 Barium Titanate (BaTiO<sub>3</sub>)

 $BaTiO_3$  - crystal structure of perovskite high-performance lead-free piezoelectric materials and their general formula is  $ABO_3$ . This perovskite crystal structure has one anion which is  $O^{2-}$  and two cations which are  $A^{2+}$  and  $B^{4+}$ . Face Centered cubic lattice (FCC) is the main skeleton of this crystal structure. The "A" cations are placed in the eight corners, while the "B" cations are placed in the mid-point and the oxygen anions are placed in the six face centers of the crystal structure. The coordination number of this structure is 12 [2, 3].

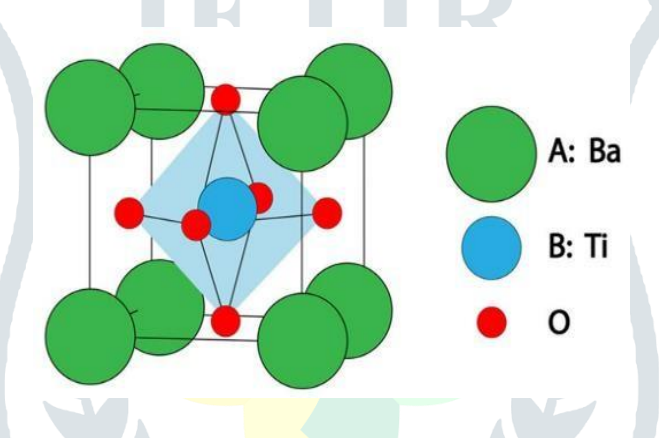


Figure 1 Structure of Barium Titanate

Good-prepared lead-free piezoelectric materials have become an important topic in the field of material science. These are LiNbO<sub>3</sub> (LN), LiTaO<sub>3</sub>(LT) and BaTiO<sub>3</sub>(BT). Among these barium titanate is the most generally used ferroelectric material and even sixty years after its discovery it has become quite significant materials for many applications like energy storage devices, dynamic random-access memory applications, actuators and tuneable capacitor devices because of these excessive dielectric constant, little loss characteristics, high permittivity, and high tunability. Lead-free material can be very interesting for environmentally friendly applications. BaTiO<sub>3</sub> which is useful in numbers known to correlate with the size and the technical tendency to reduce dimensions due to its better ferroelectric properties and excessive dielectric constant correlates this when sizes are at the Nano range. In thin film formation ferroelectric materials have been extensively studied; therefore, it is used in the application as dynamic random-access memories (DRAM) and multilayer ceramic capacitors (MLCCs) [4].

Due to its electromechanical features in addition to its ferroelectric nature BaTiO<sub>3</sub> has been widely studied, which can extensively be modified with the small amounts of variety of additives such as Sr<sup>2+</sup>, Ca<sup>2+</sup>, Sn<sup>4+</sup> and Zr<sup>4+</sup> that make them more attractive for many application [5,6,7]. In general, Zr doping to B- site (Ti) has numerous good electrical properties compared to pure BaTiO<sub>3</sub> because of its large tunability, little dielectric loss, and excessive dielectric constant. Barium zirconium titanate (BZT) has received a better deal of attention because of its good applications used in different technologies

and Ca doping at A - site increase the temperature range stability of the tetragonal phase and plays a vital in achieving the good electrical and dielectric properties of barium titanate. Currently, there is a great demand of multiferroic materials which possess the concurrently ferroelectric and magnetic ordering [8,9]. In the polymorphic phase transition, BaTiO<sub>3</sub> plays a vital in the dielectric and ferroelectric properties. Ba<sub>1—x</sub>Ca<sub>x</sub>TiO<sub>3</sub> ceramics have recently been shown to have a significant piezoelectric/electro strictive strain and numerousfunctions. In this work, the effect of Ca and Zr addition on phase structural, piezoelectric, dielectric and microstructural properties of the lead-free BCZT ceramics will be studied systematically [10,11,12].

The recent trend in electronic devices downsizing has opened the way for various nanostructured materials. Depositing ferroelectric thin films may results in a controlled crystal structure enabling desired properties. BaTiO<sub>3</sub> thin films were reported with good DC resistivity and good dielectric constant indicate an excessive dielectric nature. This has resulted significant progress in various synthesis techniques that yield more response of BaTiO<sub>3</sub> nanocrystals (NCs) with great-defined morphologies and controlled crystal phases. In this context, the preparation of new highly active, sustainable and more selective nanomaterial is of prime importance which is expected in properties of Enrichment with remarkable results in Nano size BaTiO<sub>3</sub>, BCT, BZT and their composites like BCT-BZT. Comparative study of various compositions and their different temperatures as shown in **Table 4**.



Figure. 2 Schematic representations of the two different crystalline structures of BaTiO<sub>3</sub>

#### 2. Current Status

#### 2.1 Based on single phase BaTiO<sub>3</sub>

By using the spray pyrolysis method, we have been prepared Barium Titanate (BaTiO<sub>3</sub>) thin films. This work provides a study of dielectric, structural, electrical and morphological properties of the deposited BaTiO<sub>3</sub> thin films. The XRD proved the nature of thin films is polycrystalline. X-rayphotoelectron spectroscopy (XPS) shows the better deal of the thin film's stoichiometry with BaTiO<sub>3</sub>. By using energy dispersive X-ray analysis, a presence of Ba, Ti and O in the BaTiO<sub>3</sub> thin films was observed [72, 73, 74, 75].

# 2.2 Based on Doping like Ca and Zr in $BaTiO_3$

By using the high temperature solution growth technique, single crystals of Ca doped BaTiO<sub>3</sub> have been grown with 12 and 20 mol% of calcium [169,170]. The values of dielectric constants from 150 to 450 K were measured and these values decreases with increases Ca content. The frequency increases, dielectric constant also decreases. Calcium substitution in the Ba site then increased the Curie temperature value [171,172].

BZT nanoparticles were prepared directly from solutions and study their Microstructural analysis by using XRD (X- Ray Diffraction) [13,14,15] and TEM (Transmission Electron Microscope) show that the size of material was nanoscaled like 20-25 nm in diameter, well crystallized and had perovskite crystal structure (Fig. 3 and Fig. 4) [16,17,18].

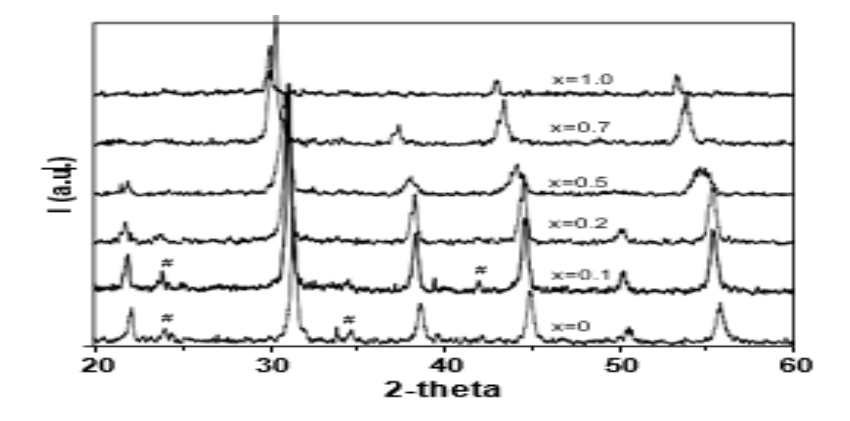


Figure. 3 XRD Pattern of Ba (Zr<sub>x</sub>Ti<sub>1-X</sub>)O<sub>3</sub> and "#" - BaCO<sub>3</sub> peaks

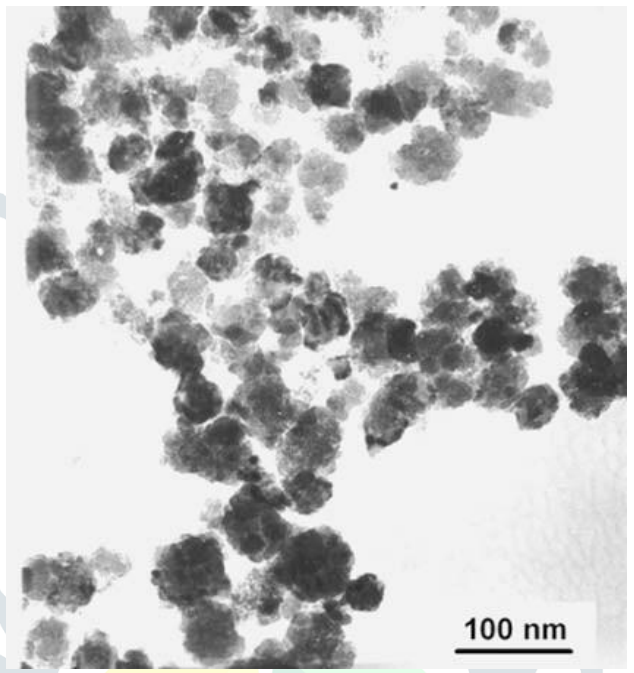


Figure. 4 TEM image of the powder of Ba(Zr<sub>0.5</sub>Ti<sub>0.5</sub>)O<sub>3</sub>

By using conventional solid state reaction method  $BaZr_xTi_{1-x}O_3$  ceramics were synthesized. X-Ray Powder diffraction technique indicates that the single phase with perovskite crystal structure. In BZT ceramics, Structural characteristics depend on Zr content increase and lattice parameters gradually increase as well. The BZT crystal structure is almost close to a cubic crystal structure when x=0.20 at room temperature [26,27,28]. The mechanical and Structural properties indicates that the lead free BZT possess excellent mechanical parameters than pure BT and is one of the most promising candidates for producing transducers, sensors and actuators which can work under load [29,30]. To determine the elastic properties like velocity of the longitudinal ultrasonic waves ( $V_L$ = 5980.9 m/s) and transverse ultrasonic waves ( $V_T$  = 3550.6 m/s) is shown in Fig. 5 [31,32]. The next Fig. 6 shows the dependence of the material constants (E, G) on zirconium concentration in BZT samples. The values of both Young's modulus (E) and the shear modulus (G) are the highest for BZT30 sample (E = 163.88 GPa and G = 66.73 GPa) [33].

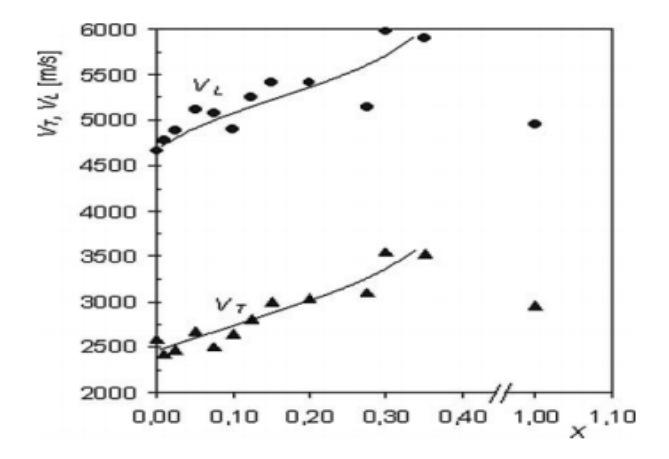


Figure. 5 Velocity of longitudinal ( $V_L$ ) and Transverse ultrasonic wave  $V_T$  of sample BZT

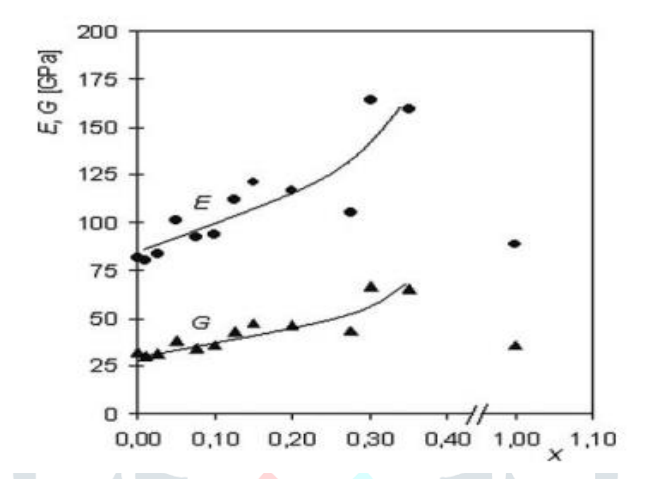


Figure. 6 Elastic constant of Young's modulus (E) and shear modulus (G) of the sample BZT

The BaZr<sub>0.05</sub>Ti<sub>0.95</sub>O<sub>3</sub> ceramics were synthesized mixed – oxide technique. In this paper, the SEM from Fig. 8 (a) shows that the average grain size of BZT sample is 250 nm, it means that grains have not grown in the sintering process with respect to the actual size of the crystallites in the BZT powders (Fig. 8 (b) [34,35,36]. X- Ray Diffraction patterns of BZT ceramic sintered at 1350°C and 1400°C as shown in Fig. 7. In XRD pattern crystallite sizes was calculated in the range of 56.3 nm to 58.9 nm from half-width of (011) peaks [37,38,39]. Fig. 9 shows the hysteresis cycle measured at room temperature and at frequency 50 Hz and by varying sintering temperature of BZT sample like 1350°C and1400°C. It indicates that the higher value of remnant polarization like 35μC/cm² and at room temperature better dielectric constant like 1700 were observed. The results assume that high-energy ball milling method is a practical method to prepare BZT because of the good dielectric and ferroelectric properties [40,41,42,43].

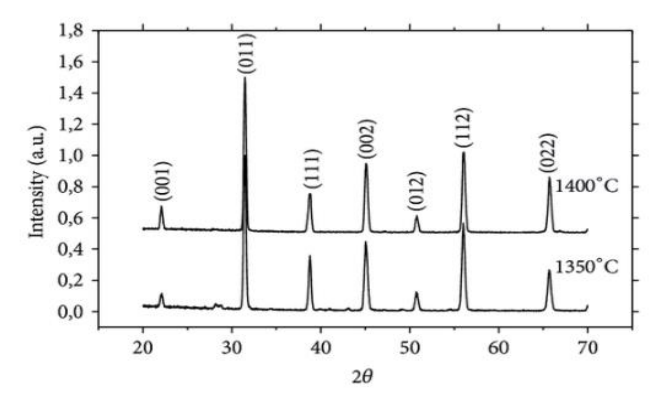
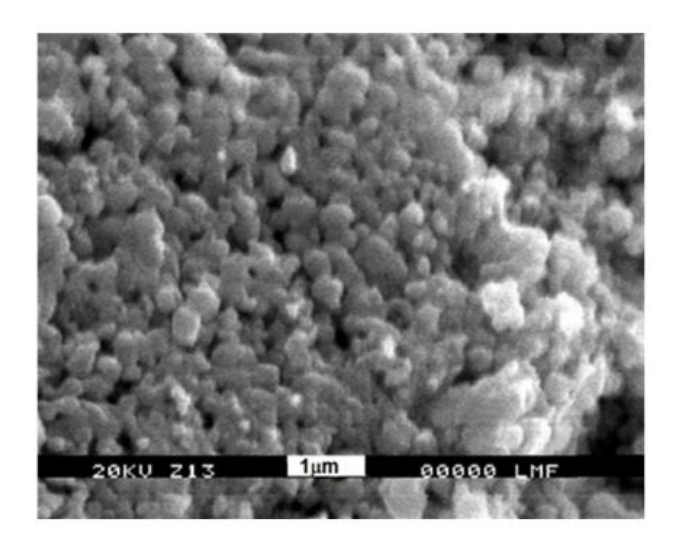


Fig. 7 XRD pattern of BZT ceramics sintered at 1350°C and 1400°C



(a)

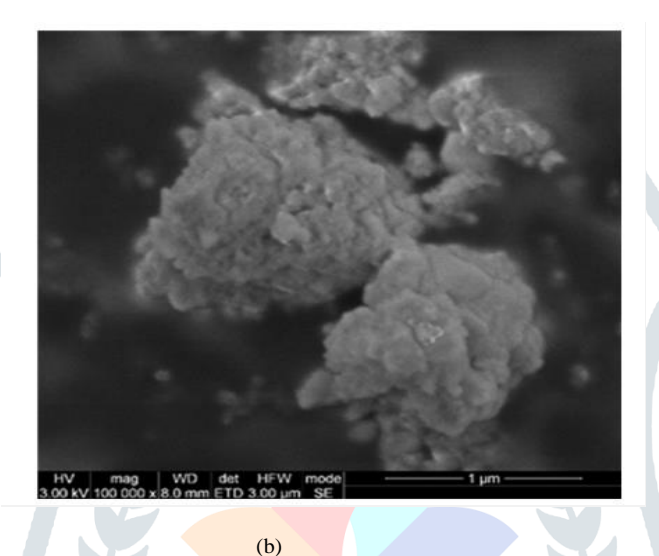


Figure. 8 (a) SEM image of the BZT sample sintered at 1350 °C (b) HRSEM image of powder BZT by 4 h

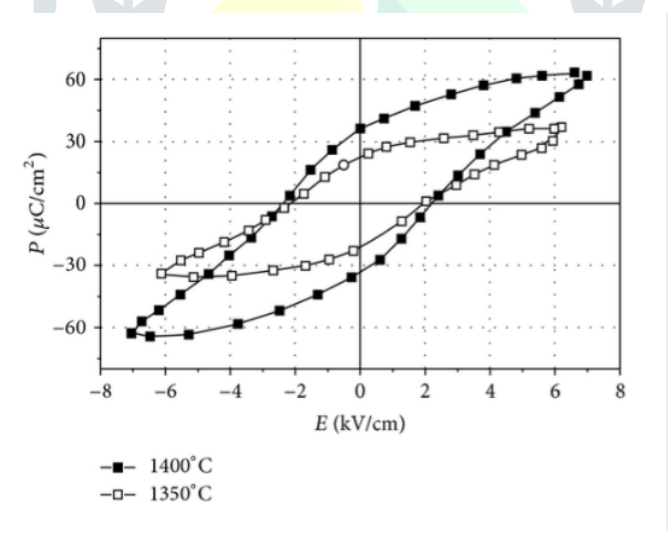


Figure. 9 Hysteresis cycle of sample BZT at 50  $H_Z$  and at room temperature sintered at 1400  $^{\circ}\mathrm{C}$ 

Ferroelectric zirconium doped barium titanate Ba  $(Zr_xTi_{1-x}O_3)$  (x=0.1, 0.2 and 0.3) was made by applying solid state method. To make single phase BZT ceramics, the mixed oxide method is used. In this work the crystal structure for x=0.1 changes from tetragonal to orthorhombic and above x=0.2 then to cubic All the samples have grain size ranging from 90.8 to 47.4 nm and ac conductivity was found maximum because of Zr content is increased [84].

In July 2018, using conventional solid-state method, the lead-free BaZr<sub>0.10</sub>Ti<sub>0.90</sub>O<sub>3</sub> was synthesized and the sample can be sintered at 1150 °C [116,117,118]. In this research paper we studied that the dielectric properties of this low-

temperature sintered samples are equivalent to pure BZT samples synthesized by applying conventional solid-state method sintering at a high temperature [119,120]. For a sample sintered at low temperature, the Curie temperature also shifts towards room temperature. [121,122,123].

Then next paper, by using a  $BaZr_{0.5}Ti_{0.5}O_3$  ceramic target, radio-frequency magnetron sputtering was used to deposit the film. In this work, the crystal structure, phase composition, and electrical properties of the prepared thin films because of substrate nature is shown to have a considerable effect [124,125,126]. The maximum tunability, n = 3, was registered for The BZT thin films obtained at Ts = 900°C, maximum tunability n=3; because of high barium content [127,128] and that time, these thin films displayed a Q-factor range 30 to 80 at a frequency of 2 GHz as shown in Fig. 10 [129,130,131].

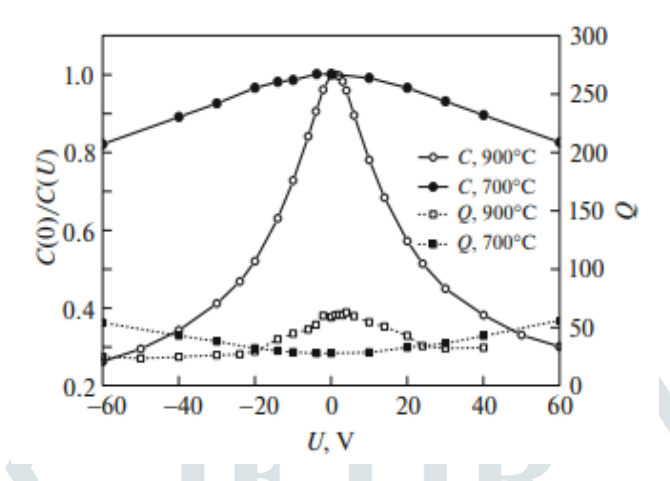


Figure. 10 Tunability and Q-factor of BZT thin films

By using magnetron sputtering, the  $BaZr_{0.2}Ti_{0.8}O_3$  thin films with different thicknesses were synthesized on substrates [132,133,134]. Combining the theoretical and experimental methods then dielectric properties of their bulk and interfacial layers are successively investigated and studied dielectric properties like dielectric constant = 891, thickness = 10.3 nm [135,136,137].

By using traditional ceramic method, BaZr<sub>1-x</sub>Ti<sub>x</sub>O<sub>3</sub> ceramics were synthesized and sintered at 1200 °C for 2h. The TEM (Transmission Electron Microscope) images indicate that Nano crystallites are agglomerated with particle size range 20 to 75.5 nm. The DC resistivity of the sample slightly decrease with increasing Ti content, whereas dielectric constant and dielectric loss rise as the Ti constant increases [138].

The next one, BZT (Barium Zirconium Titanate) was made by using the sol-gel method and at 1100°C and 1300°C under calcination and sintering temperatures a single-phase perovskite BZT was observed [139,140]. Here, we observed the amount of zirconium content increases that time the curie temperature of BaTiO<sub>3</sub> was 399 K and again increases in the zirconium content then decreased the Curie temperature to 331 K. At the phase transition, BZT had the largest dielectric constant of 19,600 [141,142]. Fig. 11 shows that XRD Pattern of BZT sample that confirm the formation of the pure perovskite crystal structure of BZT without second phase. Fig. 12. Shows that the grains sizes are irregular and an average grain size range 10–30 µm [143,144]. **Table 3** indicates that the good dielectric constant [145,146].

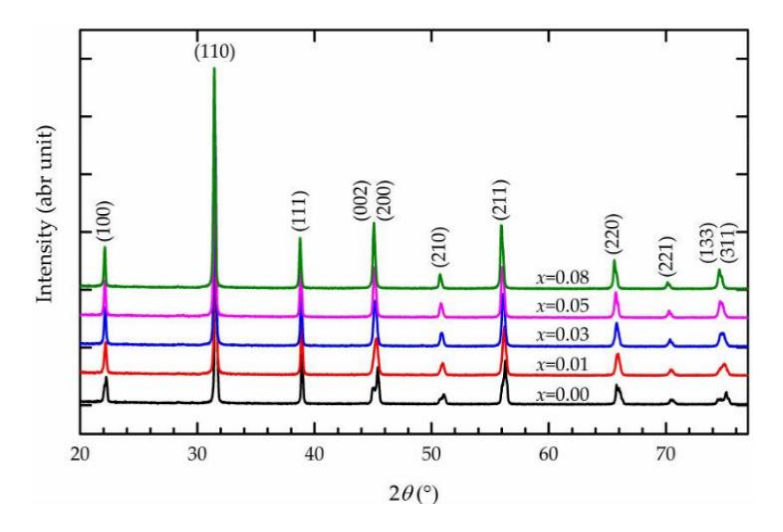


Figure. 11 X Ray Diffraction Pattern of BZT sample

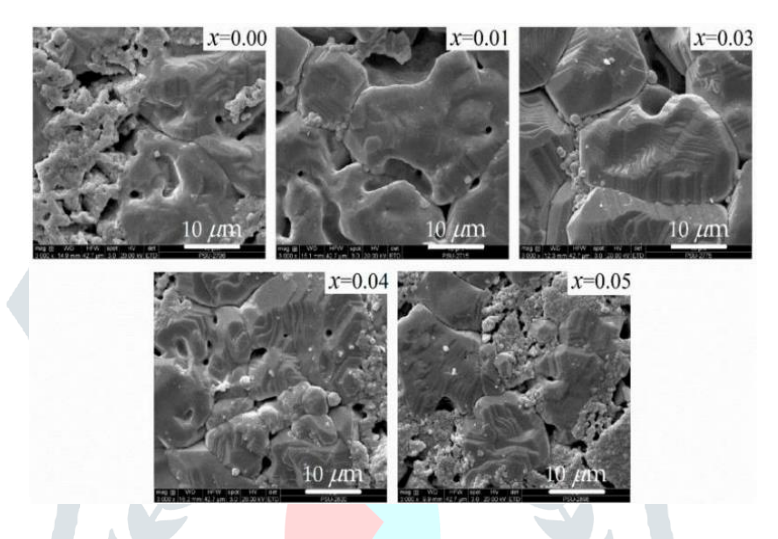


Figure. 12 SEM image of the sample BZT

By using a mixed oxide method, barium zirconium titanate (BaZr<sub>0.05</sub>Ti<sub>0.95</sub>O<sub>3</sub>) ceramics were synthesized and study their properties [147,148,149,150]. The cement based BZT piezoelectric composite modified with PVDF can enhance the dielectric, physical and ferroelectric properties [151,152,153]. The SEM images indicates that increasing densities =3.81 g/cm<sup>3</sup> and decreasing porosities =10.57 % can be obtained with increasing PVDF content [154,155,156].

The Pure BZT ceramics were prepared by using the ball milling method and operation has a significant influence on sintering conditions was observed. Single-phase BZT was obtained under sintering temperature at 1350°C and the average crystallite size was determined as 79.2 nm by using the Scherrer formula [157,158,159]. The TG-DTA and DTG curves obtained for the samples BZT and in the TGA of BZT powder, the total weight loss of about 1.73% as shown in Fig. 13[160,161,162]. Fig. 14 shows the FT-IR spectra at room temperature of BZT powder and the results of the FT-IR spectra are compatible with XRD and TGA-DTA analysis, confirming that the formation temperature of BZT powder is over 1200°C [163,164,165,166].

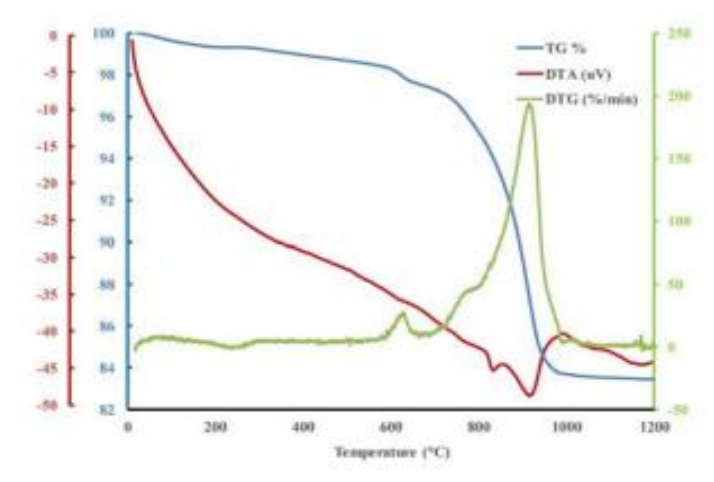


Figure. 13 TG-DTA and DTG curves of BZT sample

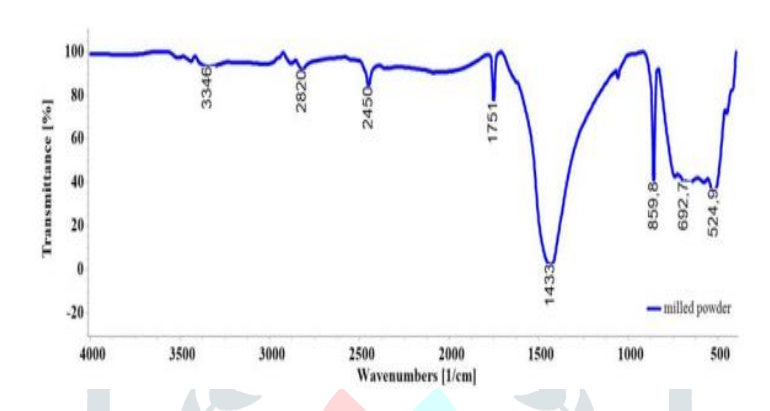


Figure. 14 FT-IR spectrum of BZT Sample

Then doping of both Ca and Zr in BaTiO<sub>3</sub>, the solid – state reaction technique is used to synthesized, (Ba<sub>1-x</sub>Ca<sub>x</sub>) (Ti<sub>0.9</sub>Zr<sub>0.1</sub>)O<sub>3</sub> ceramics [19,20,21]. At normal temperature, XRD data in the range 0.14< x <0.18 proves that the trigonal and orthorhombic phases and also sample shows pure perovskite crystal structure (Fig. 15). For this sample of x=0.16, improved piezoelectric and dielectric properties like that piezoelectric constant (d<sub>33</sub>) =328 pC/N, the planar electromechanical coupling factor ( $k_p$ ) =37.6% and dielectric constant ( $\epsilon$ ') =4800 [22,23]. Fig. 16 shows the hysteresis cycle of P-E field of BCZT sample. At Ca content increases then the EC(coercive fields) value increases and also P<sub>r</sub>( remnant polarization) values increases to a maximum value and then decreases of sample BCZT at x=0.12, x= 0.14, x= 0.16 and x=0.18 [24,25].

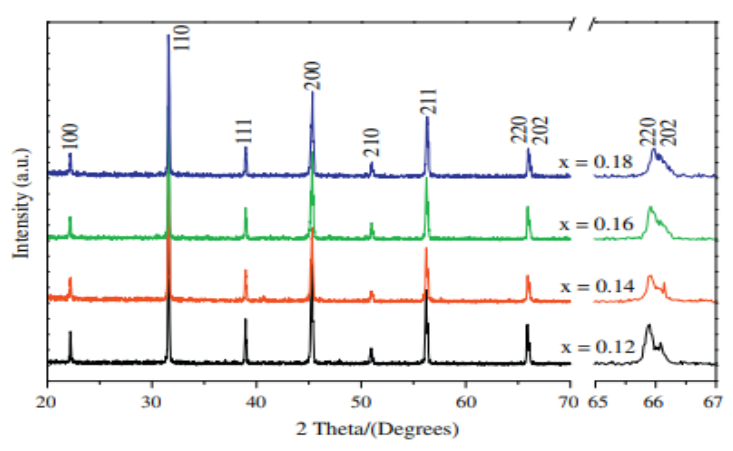


Fig. 15 XRD pattern of sample BCZT

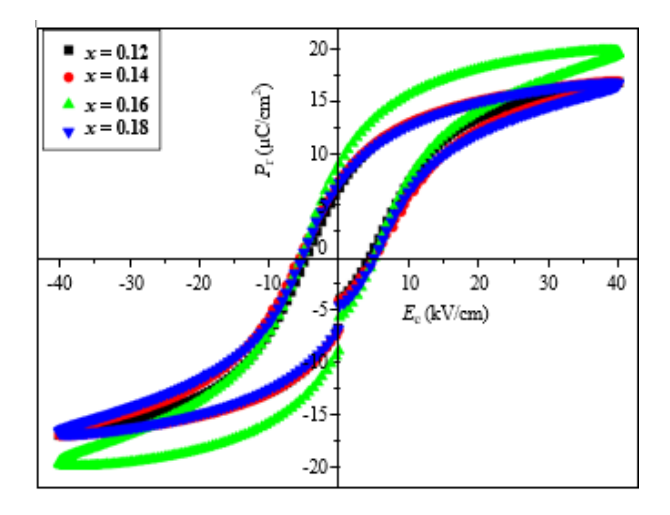


Fig. 16 Hysteresis loop of (P-E) of the sample BCZT at room temperature

#### 2.3 Based on BCT-BZT composite

The BZT-BCT (Barium Zirconium Titanate-Barium Calcium Titanate) thin film was made by using sol-gel method. With the help of the nano indentation technique and to studied their nano mechanical features, structural properties and nanomechanical properties [44,45,46]. The thin film of BZT-BCT sample has comparatively excessive residual stress of 1.66 GPa and measured very good elastic properties [47,48,49]. Fig. 17 shows that hysteresis cycle (P-E) was measured the remnant polarization value ( $P_r = 10 \,\mu\text{C/cm}^2$ ) and coercive field value ( $V_C = 5V$ ) [50,51,52,53].

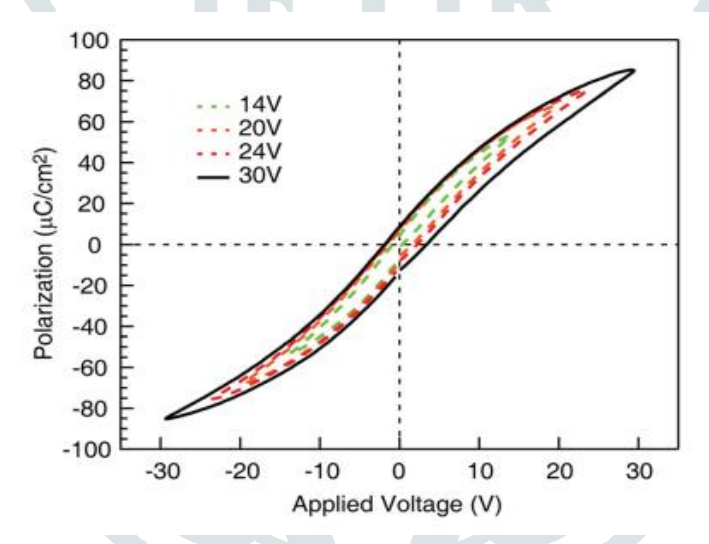


Figure. 17 Hysteresis cycle of BZT-0.5BCT thin films

The  $0.5Ba(Zr_{0.2}Ti_{0.8})O_3$ -  $0.5(Ba_{0.7}Ca_{0.3})TiO_3$  thin films was made by the solid-state reaction technique. The structural and ferroelectric properties of 0.5BZT - 0.5BCT thin films were studied [76,77,78]. Fig.18 shows that at different pulse repetition rates the frequency dependence of the dielectric permittivity ( $\varepsilon_r$ ) and dielectric loss (tg)of 0.5BZT-0.5BCT thin films were grown [79,80]. The dielectric permittivity is 265 at 1 kHz and the dielectric loss value 0.2 [81,82,83].

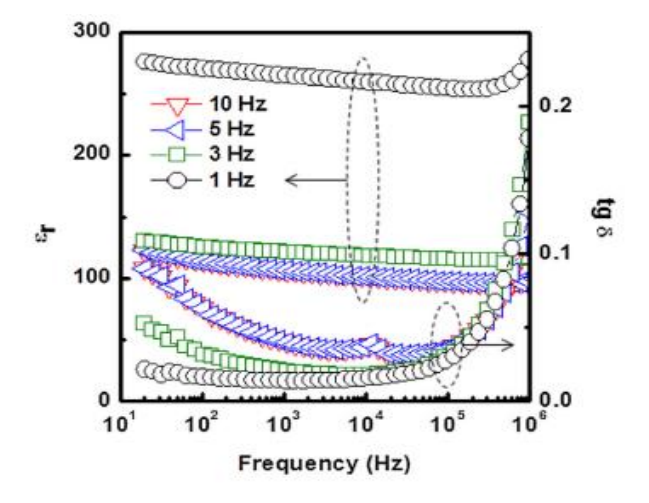


Figure.18. Diagram of dielectric permittivity and dielectric loss versus frequency of 0.5BZT-0.5BCT thin films

By using electrospinning technique 0.5Ba(Zr<sub>0.2</sub>Ti<sub>0.8</sub>)O<sub>3</sub>-0.5(Ba<sub>0.7</sub>Ca<sub>0.3</sub>)TiO<sub>3</sub> Nano composites were synthesized and the PVDF-based composites filled by the BT NPs or BZT-BCTNFs were produced [99,100,101]. The dielectric constant of the BZT-BCT NFs/PVDF composite was observed all time higher than that of BT NPs/PVDF composite [102,103,104]. The X-ray diffraction and SEM techniques show the evidence that BZT- BCT NFs had a pseudo- cubic structure. The energy density and efficiency of 3 vol% BZT- BCT NFs/PVDF composites is 3.08 J/ cm<sup>3</sup> at 240 kV/mm and 60.56% respectively [105,106]. These results also provide a simple and effective method to achieve the materials with high capacitance for energy storage [107,108,109].

By using solid-state reaction method, the lead- free ferroelectric with composition (0.55)Ba<sub>0.92</sub>Ca<sub>0.08</sub>TiO<sub>3</sub>-(0.45)BaTi<sub>0.96</sub>Zr<sub>0.04</sub>O<sub>3</sub> was prepared and studied there structural, dielectric, ferroelectric and piezoelectric properties [110,111]. By using XRD Patterns and Raman spectra analysis indicates the two ferroelectric phase's tetragonal and orthorhombic crystal structure [112,113]. In the present work, the prepared lead-free solid (0.55)BCT-(0.45)BZT ceramic shows better properties and it can be used for different applications like permanent ferroelectric memory, piezoelectric sensor, capacitor, etc [114,115].

## 2.4 Based on the Different composite

The modified Pechini method and spin coating methods were used to synthesized LSMO and BaZr<sub>0.15</sub>Ti<sub>0.85</sub>O<sub>3</sub> thin film heterostructures [54,55,56]. In the present work, the analysis indicates that the dielectric properties of the magneto-dielectric (MD) heterostructures indicate the presence of electrode effect and interfacial polarization and the AC conductivity increases as the applied magnetic field increases, due to the negative CMR effect of LSMO [57,58]. It is obtained that the MD is negative at low frequencies and becomes positive for frequencies above 60 kHz [59,60,61].

Then the next, by using solid-state reaction technique Ceramic composites of mullite / BZT were synthesized [62,63,64]. In this research paper presents the effect of BZT addition on phase formation then increasing BZT content it gives good electrical properties, remnant polarization, dielectric constant and piezoelectric coefficient [65,66,67]. The good ferroelectric properties of the BZT phase were obtained [68,69]. Fig. 19 shows that the Scanning electron Microscope (SEM) were observed microstructure and (EDS) energy-dispersive X-ray spectroscopy detect the Ba, Ti, O and Mullite elements [70,71].

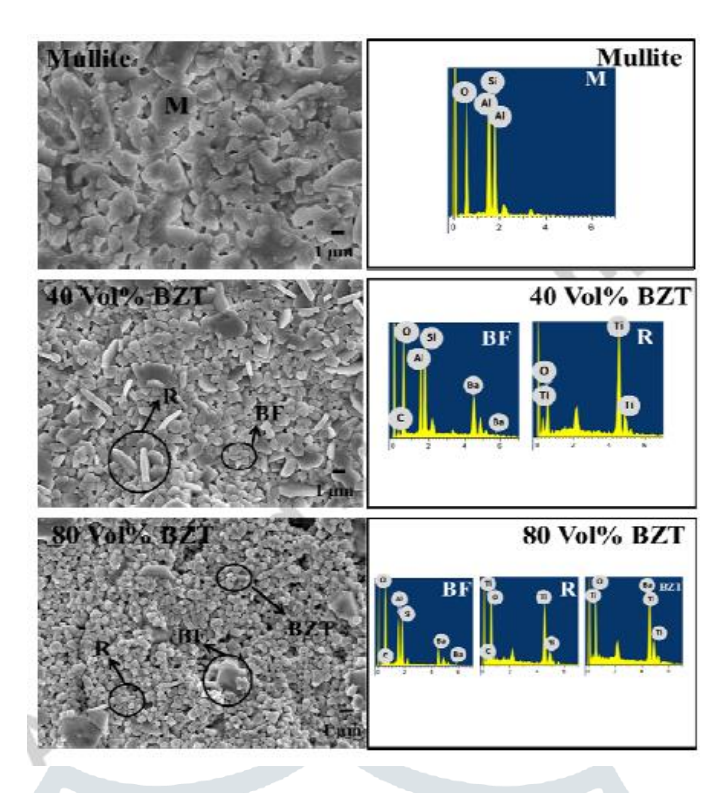


Figure. 19 SEM micro image and EDS result

(M: mullite, BF: barium feldspar, R: rutile)

By using the standard solid-state method (Ba<sub>0.02</sub>Ca<sub>0.08</sub>- TiO<sub>3</sub>) and Fe-doped BCT ceramics were successfully prepared. In the present research work XRD and SEM indicates the average crystallite size is between 40 nm and 80 nm then Fe – doping induced a decrease in the grain size. Because of FE-doping effect, the dielectric constant and dielectric loss follow the usual dielectric dispersion behavior and the Curie temperature (Tc) has been increased from 120 °C for BT to 135 °C BCT [85,86]. Fig. 20 shows that the hysteresis cycle polarization versus electric field (P-E) of BT, BCT8, and Fe-doped BCT8 and it confirm the ferroelectric nature of these sample [87,88,89]. **Table 1** indicates that the values of the coercive electric field (E<sub>c</sub>), remnant polarization (P<sub>r</sub>) and maximum polarization (P<sub>max</sub>) for all the samples are determined and compared [90,91] and **Table 2** shows the room temperature values of  $\varepsilon'$  and tan  $\delta$  at high frequency [92,93].

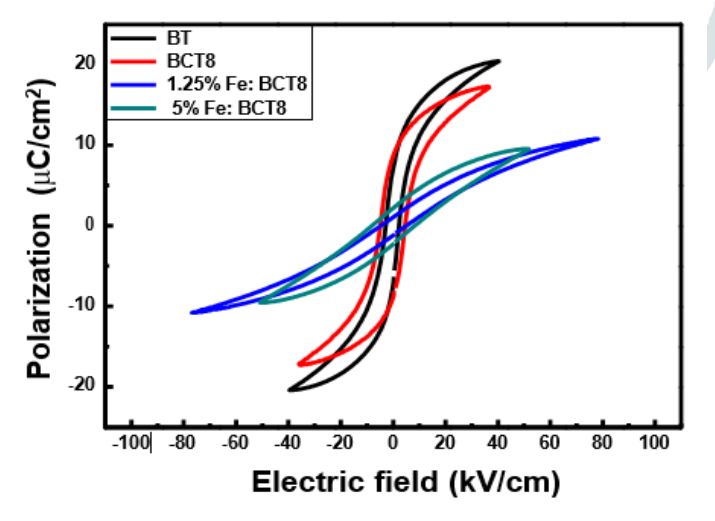


Figure. 20 The hysteresis cycle (P-E) of the samples BT, BCT8, and Fe-doped BCT8

By applying the conventional solid state reaction method the  $(La_xBa_{1-x})(Ti_{0.8}Zr_{0.2})O_3$ , (x=0.01,0.02,and0.03) ceramics were prepared. In BZT dielectric properties suggested a diffuse phase transition. X-ray powder diffraction and SEM shows that predominantly single-phase microstructure [94,95,96]. In this work increase in La doping introduced relaxor

properties but FWHM was lowered and it can be concluded that the broadest phase transition in  $(La_xBa_{1-x})(Ti_{0.8}Zr_{0.2})O_3$  ceramic is obtained for a low La doping, which is important for capacitor applications [97,98].

#### 3 CONCLUSIONS AND FUTURE PERSPECTIVES

Piezoelectric and ferroelectric ceramics are most important and widely used in variety of technologies. Different types of applications like audio delay lines, sonar, high voltage amplifiers, ultrasonic cleaning, medical ultrasound applications, phonograph pickups, bandpass filters and oscillator frequency control in communications equipment industrial non-destructive inspection, watches and accelerometers are included [1]. Many new applications have arrived with the development of ceramic processing and thin film technology like multilayer ceramic capacitors (MLCCs), piezoelectric actuators and positive temperature coefficient resistors (PTCRs), ferroelectric thin films for non-volatile memories, electro-optical device and for humidity sensors based on nano-BaTiO<sub>3</sub> composite material. Currently in 2011, Y.-H. Chen et al. reported that synthetic nano-BTO and nano-STO can be used to remove Cu<sup>2+</sup> from aqueous solutions and thus have potential applications in environmental protection agents [3].

In the last eight decades, there has been hard work in the growth of Pb-free barium titanate-based piezo electrics and their study has been spread across basic, applied research, the future markets and the development of prototype devices where we estimate that this type of material offers comparable advantages. The paper thoroughly discussed the following results, By using the high temperature solution growth technique, single crystals of Ca doped BaTiO<sub>3</sub> have been grown with 12 and 20 mol% of calcium [169,170]. The values of dielectric constants from 150 to 450 K were measured and these values decreases with increases Ca content. The BZT (Barium Zirconium Titanate) nanoparticles - directly from solutions and study their (Micro) structural analysis by using TEM (Transmission Electron Microscope) and XRD (X-Ray Diffraction) show that the material was Nano scaled like 20 to 25 nm in diameter, well crystallized and had a perovskite crystal structure. By using conventional solid state reaction method BaZr<sub>x</sub>Ti<sub>1-x</sub>O<sub>3</sub> ceramics were synthesized. To determine the elastic properties like velocity of the longitudinal ultrasonic waves ( $V_L = 5980.9 \text{ m/s}$ ) and transverse ultrasonic waves ( $V_T = 3550.6 \text{ m/s}$ ) m/s) and The values of both Young's modulus (E) and the shear modulus (G) are the highest for BZT sample (E = 163.88GPa and G = 66.73 GPa) and by varying sintering temperature of BZT sample like 1350°C and 1400°C. It indicates that the higher value of remnant polarization like 35µC/cm<sup>2</sup> and better dielectric constant like 1700 were observed. The doping of both Ca and Zr in BaTiO<sub>3</sub>, the solid – state reaction technique is used to synthesized, (Ba<sub>1-x</sub>Ca<sub>x</sub>) (Ti<sub>0.9</sub>Zr<sub>0.1</sub>)O<sub>3</sub> ceramics. For this sample of x=0.16, improved piezoelectric and dielectric properties like that piezoelectric constant (d<sub>33</sub>) =328 pC/N, the planar electromechanical coupling factor  $(k_p) = 37.6\%$  and dielectric constant (E') = 4800. The hysteresis cycle of P-E field of BCZT sample. At Ca content increases then the E<sub>C</sub> (coercive fields) value increases and also P<sub>r</sub> (remnant polarization) values increases to a maximum value and then decreases.

The cement based BZT piezoelectric composite modified with PVDF can enhance the dielectric, physical and ferroelectric properties. The SEM images indicates that increasing densities =3.81 g/cm³ and decreasing porosities =10.57 % can be obtained with increasing PVDF content. The Pure BZT ceramics were prepared by using the ball milling method and Single-phase BZT was obtained under sintering temperature at 1350°C and the average crystallite size was determined as 79.2 nm by using the Scherrer formula. The TG-DTA and DTG curves obtained for the samples BZT and in the TGA of BZT powder, the total weight loss of about 1.73%. The Fe-doped BCT ceramics – by the solid-state reaction. XRD (X-Ray Powder Diffraction) and SEM (Scanning Electron Microscope) indicates the average crystallite size is between 40 nm and 80 nm and Curie temperature (Tc) has been enhanced from 120 °C to 135 °C because of Fe – doping in Barium Calcium Titanate.

These observed properties of composite material indicate that the lead-free BaTiO<sub>3</sub>, BZT and BCT is suitable for different applications like capacitor, piezoelectric sensor and ferroelectric memory device etc. Currently, the preferred choice for capacitor applications are barium titanate-based materials.

#### 4 ACKNOWLEDGMENT

Sadhana R. Salunkhe is thankful to the SARTHI (CSMNRF) for their Financial Support. This work was supported by my guide Dr. S. A. Patil, and Co – guide Dr. L. D. Jadhav and I am also thankful to my family members and Friends for their great support.

#### 5 CONFLICT OF INTEREST

1) The authors declare that they have no known competing financial interests or personal relationships that could have appeared to influence the work reported in this paper.

#### 6 Author Contribution

Salunkhe S. R.: performed the experiments, characterization, data analysis, research discussion and manuscript preparation. Patil S. A. and Jadhav L. D. provided the supervision, research discussion and reviewed the manuscript. All authors have read and agreed to the published version of the manuscript.

## 7 References

- 1) S. Ahmad, R. K. Panda, and V. F. Janas,
  - "Ferroelectric ceramics: processing, properties & applications" 2006
- 2) K. I. Osman
  - Synthesis and characterization of BaTiO<sub>3</sub> ferroelectric material, Thesis of BaTiO<sub>3</sub>, 2011
- 3) D. W. Richerson
  - "Modern ceramic engineering: Properties, processing, and use in design", Second Edition, Marcel Dekker, inc., (1992)
- 4) M. Acosta, N. Novak, V. Rojas, S. Patel, R. Vaish and J. Koruza etc.
  - J. Appl. Phys. Rev. 4 (2017) 041305
- 5) B. Shen, Q. Zhang, J. Zhai and Z. Xu
  - J. Ceram. Int. 39 (2013) S9-S13
- 6) P. Julphunthong, S. Chootin and T. Bongkarn
  - J. Ceram. Int. 39 (2013) S415-S419
- 7) T. Mazon, M. A. Zaghete, J. A. Varela and E. Longo
  - J. Euro. Ceram. Soc. 27 (2007) 3799-3802
- 8) M. M. Vijatovi'c, J. D. Bobi'c and B. D. Stojanovi'c
  - J. Sci. Sinter. 40 (2008) 155-165
- 9) I. Levin, V. Krayzman and J. C. Woicik
  - J. Appl. Phys. Lett. 102 (2013)162906
- 10) W. F. Liu and X. B. Ren
  - J. Phys. Rev. Lett. 103 (2009) 257602
- 11) J. L. Zhang, X. J. Zong and L. Wu
  - J. Appl. Phys. Lett. 95 (2009) 022909
- 12) L. L. Zhang, X. S. Wang, H. Liu and X. Yao
  - J. Am. Ceram. Soc. 93 (2010) 1049
- 13) J. Q. Qi, Y. Wang, W. P. Chen, L. T. Li, and H. L. W. Chan
  - Journal of Nanoparticle Research 8 (2006) 959 963
- 14) Bottcher R., C. Klimm, D. Michel, H. C. Semmelhack, G. Volkel and H. J. Glasel etc.
  - Phys. Rev. B. 62 (2000) 2085 2095
- 15) Fery M. H. and D. A. Payne
  - Appl. Phys. Lett. 63 (1993) 2753 2755
- 16) Hernandez B. A., K. S. Chang, E. R. Fisher and P. K. Dorhout
  - Chem. Mater. 14 (2002) 480-482

- Slamovich E. B. and I. A. Aksay
   J. Am. Ceram. Soc. 79 (1996) 239-247
- 18) Morrison F., Y. Luo, I. Szafraniak, V. Nagarajan, B. Wehrspohn, M. Steinhart and J. F. Scott Adv. Mater.Sci. 4 (2003) 114-122
- 19) W. Li, Z. Xu, R. Chu, P. Fu and G. Zang Journal of Physica B. 405 (2010) 4513 – 4516
- 20) J. L. Zhang, X. J. Zong and L. Wu Appl. Phys. Lett. 95 (2009) 022909
- 21) P. Z. Zhang, M. R. Shen, L. Fang, F. G. Zheng, X. L. Wu, J. C. Shenand H. T. Chen Appl. Phys. Lett. 92 (2008) 222908
- 22) P. Kantha, K. Pengpat, P. Jarupoom Curr. Appl. Phys. 9 (2009) 460
- 23) Z. Yu, R. Y. Guo, A. S. Bhalla J. Appl. Phys. 88 (2000) 410
- P. S. Dobal, A. Dixit, R. S. Katiyar
   J. Appl. Phys. 86 (2001) 8085
- P. S. R. Krishna, D. Pandey, V. S. Tiwari and R. Chakravarthy
   Appl. Phys. Lett. 62 (1993) 231
- B. Garbarz Glos, K. Bormanis, A. Kalvane and I. Jankowska-Sumara,
   J. Integrated Ferroelectrics. 123 (2011) 130 136
- H. Y. Tian, Y. Wang, J. Miao, H. L. W. Chan and C.L. Choy
   J. Alloys Comp. 431 (2007) 197 -202
- 28) V. V. Shvartsman, J. Zhai and W. Kleemann Ferroelectrics 379 (2009) 77 - 85
- 29) N. Nanakorn, P. Jalupoom, N. Vaneesorn and A. Thanaboonsombut Ceram. Internat. 34 (2008) 779-782
- 30) Y. L. Wang, L. T. Li, J. Q. Qi and Z. L. Gui Ceram. Internat. 28 (2002) 657-661
- 31) B. Garbarz-Glos, W. Smiga, W. Suchanicz and R. Bujakiewicz-Koronska Integrated Ferroelectrics. 108 (2009) 67-76
- 32) J. PiekarczykInz. Mater. 13 (1992) 72-73
- J. Piekarczyk, H. W. Hennicke and R. Pampuch Ber.D.K.G. 59 (1982) 227-232
- 34) A. Frattini, A. Di. Loreto and O. De. Sanctis Journal of Materials. 6 (2013) 393017
- 35) S. Lee, M. Kwak, S. Moon, H. Ryu, Y. Kim and K. Kang Integrated Ferroelectrics. 77 (2005) 93-99
- 36) L. B. Kong, J. Ma, H. Huang, R. F. Zhang and W. X.Que Journal of Alloys and Compounds. 337 (2002) 226 230
- U. Weber, G. Greuel, U. Boettger, S. Weber and R. Waser
   J. American Ceram. 84 (2001) 759-766
- K. -i. Mimura, T. Naka, T. Shimura, W. Sakamoto and T. Yogo
   J. Thin Solid Films. 23 (2008) 8408-8413
- C. B. Reid, J. S. Forrester, H. J. Goodshow and E. H. Kisi
   J. Ceram. Internal. 6 (2008) 1551-1556
- 40) C. Gomez-Yanez, C. Benitez and H. Balmori-Ramirez

- J. Ceram. Internal. 3 (2000) 271-277
- 41) T. Maiti, R. Guo and A. S. Bhalla
  - J. American Ceram. 6 (2008) 1769-1780
- N. Nanakorn, P. Jalupoom, N. Vaneesorn and A. Thanaboonsonbut
   J. Ceram. Internal 4 (2008) 779-782
- 43) V. Berbenni, A. Marini and G. Bruni
  - J. Thermochimica Acta. 2 (2001) 151-158
- 44) Z. M. Wang. Zh. L. Cai, K. Zhao, X. L. Guo, J. Chen and Zh. G. Liu J. Applied physics letters. 103 (2013) 071902
- 45) X. J. Zheng, Z.Y. Yang and Y. C. ZhouScr. Mater. 49 (2003) 71
- J. E. Bradby, J. S. Williams and M. v. Swain
   J. Mater. Res. 19 (2004) 380
- 47) M. A. Alguero, J. Bushby, M. J. Reece and A. Srifert Appl. Phys. Lett. 81 (2002) 421
- 48) W. Liu and X. RenPhys. Rev. Lett. 103 (2009) 257602
- A. M. Minor, E. T. Lilleodden, M. Jin and W. Morris Jr. Philos. Mag. 85 (2005) 323
- 50) Y. IkuharaJ. Ceram. Soc. Jpn. 110 (2002) 139
- 51) K. Yao, S. H. Yu and F. E. H. Tay Appl. Phys. Lett. 82 (2003) 4540
- 52) X. J. Zheng, Y. C. Zhou and J. J. Li Acta. Mater. 51 (2003) 3985
- 53) W. H. Xu, D. Lu and T. Y. Zhang Appl. Phys. Lett. 79 (2001) 4112
- 54) A. N. Tarale, D. J. Salunkhe, P. B. Joshi and S. B. Kulkarnia J Mater Sci. Mater Electron 24 (2013) 4457 – 4463
- 55) S. Mahajan, O. P. Thakur, C. Prakash, K. Sreenivas
  - Mater. Sci. 34 (2011) 1483
- F. Mouraa, A. Z. Simoesb, C. A. Paskocimasa, M. A. Zaghetea and J. A. Varelaa etc. Mater. Chem. Phys. 123 (2010) 772
- 57) L. P. Curecheriu, R. frunza and A. Ianculescu
  - Appl. Ceram.2 (2008) 81
- 58) A. Dixit, S. B. Majumdar, A. Savvinov and A. S. Bhalla
  - J. Mater. Lett. 56 (2002) 933
- 59) Z. Ying, P. Yun, D. Y. Wang, X. Y. Zhou and H. L. W. han
  - J. Appl. Phys. 101 (2007) 086101
- 60) A. N. Tarale, Y. D. Kolekar, V. L. Mathe and P. Joshi
  - Electron. Mater. Lett. 8 (2012) 381
- 61) S. S. Veer, D. J. Salunkhe, S. V. Kulkarni and P. B. Joshi
  - J. Eng. Mater. Sci. 15 (2008) 121
- 62) N. Lertcumfu, K. Pengpat, S. Eitssayeam, T. Tunkasiri, and G. Rujinakul J Ceramics International. 03 (2015) 191

- H. S. Tripathi, A. Dhose, M.K. Halder and H. S. MaitiBull. Mater. Sci. 35 (2012) 639-643
- 64) Z.Yu, C.Ang, R. Guo and A.S. Bhalla, J.appl. phy. 92 (2002) 489-1493
- 65) C. Xin, H. Shifeng and C. Jun J.appl.phy. 101 (2007) 094110
- 66) W. Li, Z. Xu, R. Chu, P. Fu and G. Zang, Mate. Lett. 64 (2010) 2325–2327
- 67) V. Viswabaskaran, F.D. Gnanam and M. Balasubramanian Ceram. Int. 29 (2003) 564-571
- 68) M.A. Sainz, F.J. Serrano, J.M. Amigo and J. Bastida

  J Eur Ceram Soc 20 (2000) 403-412
- 69) B.M. Kim, Y.K. Cho, S.Y Yoon and H.C. Park Ceram. Int. 35 (2009) 579-583
- J. AnggonoJ. teknikmesin 7 (2005) 1-10
- J.W. Kim, H. Shima, K. Nishida and T. YamamotoJ. Korean Phys. Soc. 65 (2014) 275-280
- 72) F. JOMNI, P. GONON, F. E. KAMEL, B. YANGUI Integr. Ferroelectr. 97 (2008) 121
- 73) T. XU, J. WANG, T. SHIMADAJ. Phys.-Condens. Mat. 25 (2013) 415901
- 74) S. S. Shinde and C. H. BhosaleJ. Photoch. Photobio.B, 120 (2013) 1
- 75) J. WU and J. WANGJ. Appl. Phys. 110 (2011) 064104
- J. P. Silva, K. Kamakshi, K. C. Sekhar, X. R. Novoa, E, C. Queiros and J. Agostinho Moreira, etc Journal of the European Ceramics Society. 09 (20165) 011
- 77) B. C. Luo, D. Y. Wang, M. M. Duon and S. Li Appl. Phys. Lett. 103 (2013) 122903
- 78) W. L. Li, T. D. Zhang, D. Xu, Y. F. Hou, W. P. Cao and W. D. Fei J. Eur. Ceram. Soc. 35 (2015) 2041-2049
- 79) Y. Lin, G. Wu, N. Qin and D. Bao
  Thin Solid Films 520 (2012) 2800-2804
- 80) K. C. Sekhar, A. Nautiyal and R. NathJ. Appl. Phys. 105 (2009) 024109
- S. Sharma, M. Tomar, A. Kumar, N. K. Puri and V. Gupta
   J. Appl. Phys. 118 (2015) 074103

82) Y. Guo, K. -I. Kakimoro and H. Ohsato

Mater. Lett. 59 (2005) 241-244

83) Q. Lin, D. Wang and S. Li

J. Am. Ceram. Soc. 98 (2015) 2094-2098

84) H. H. Singh, A. D. Sharma and H. B. Sharma

Int.J. Eng. Tech., Management and Applied Sciences (2017) 2349 - 4476

85) B. C. Keswani, R. S. Deven, R. C. Kamble and A. R. James Journal of Alloys and Compounds. 712 (2017) 320 –333

86) J. F. Scott, Nat.Mater. 6 (2007) 256-257

M. Bibes and A. BarthélémyNat. Mater. 7 (2008) 425-426.

88) . A. Benedek and C.J. FennieJ. Phys.Chem. C 117 (2013) 13339-13349

89) P.K. PandaJ. Mater.Sci. 44 (2009) 5049-5062

90) M.B. Smith, K. Page, T. Siegrist and P.L.J. Am. Chem. Soc. 130 (2008) 6955-6963

M. M. Vijatović, J.D. Bobić, and B.D. Stojanović
 Sci. Sinter. 40 (2008) 155-165.

F. Lin, D. Jiang, X. Ma, and W. ShiJ. Mag. Mag. Mater. 320 (2016) 691-694

93) C.-X. Li, B. Yang, S.-T. Zhang, D.-Q. Liu, R. Zhang and Y. Sun, J. Alloys Comps 590 (2014) 346-354

94) R. Kumar, K. Asokan, S. Patnaik and Balaji Birajdar Journal of ferroelectrics. 517 (2017) 8 – 13

95) V. V. Shvartsman and D. C. LupascuJ. of the American Ceramic Society. 95 (2012) 1 -26

96) S. Ghosh, M. Ganguly, S.Rout and T.Sinha The European Physical Journal Plus 130 (2015) 1 -18

97) R. Kumar, K. Asokan, S. Patnaik and B. Birajdar Journal of Alloys and Compounds 687 (2016) 197 – 203

98) W. Cai, C. Fu, J. Gao and H. Chen Journal of Alloys and Compounds. 480 (2009) 870 –873

99) Q. Chi, G. Liu, C. Zhang, Y. Cui, X. Wang, Q. LeiJ. Result in Physics 8 (2018) 391 – 396

100) Li Q, Chen L, Gadinski MR, Zhang S, Zhang G, Li H, and Haque A. etc. Nature. 9 (2015) 523 – 576

101) Dang ZM, Yuan JK, Yao SH and Liao R J. Adv. Mater. 665 (2013) 6334

102) Chi Q, Ma T, Zhang Y, Cui Y, Zhang C and Lin J. etc. J. Mater. Chem. A. 66 (2017)16757

103) M.K. Arun, G.M. Treich, T.D. Huan, R. Ma, M. Tefferi and Y. Cao, etc Adv. Mater, 28 (2016) 6277-6291

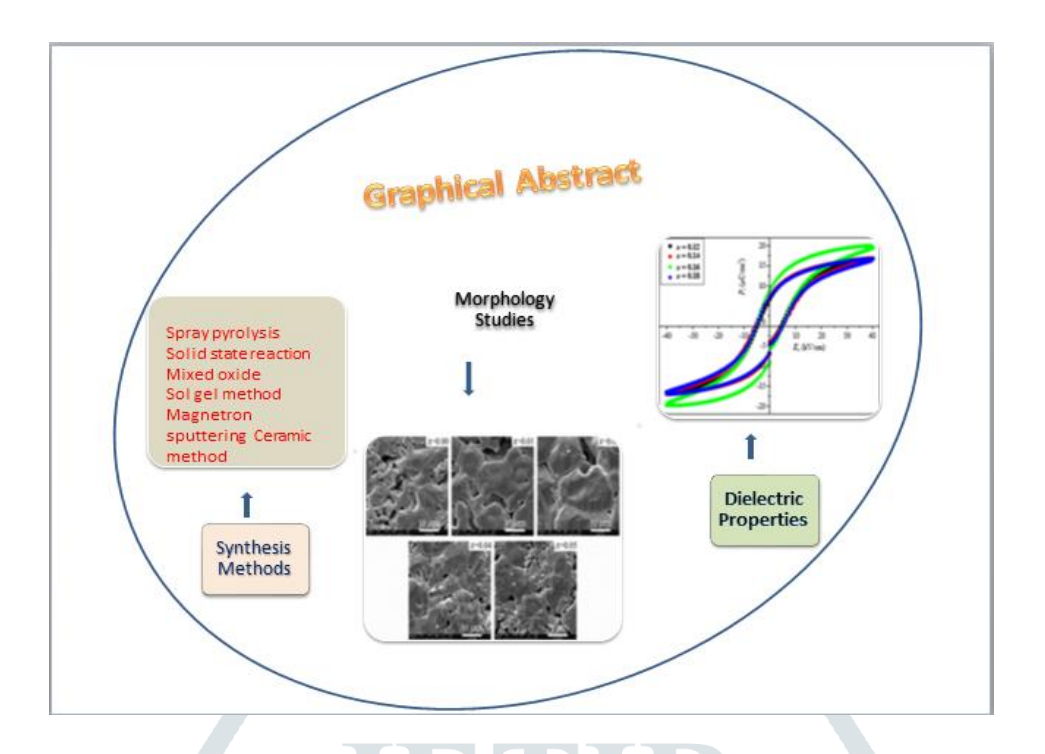
- 104) W.H. Yang, S.H. Yu, R. Sun and R.X. Du Acta Mater. 59 (2011) 5593-5602
- 105) Q.G. Chi, J.F. Dong, C.H. Zhang, C.P. Wong, X. Wang and Q.Q. Lei J. Mater. Chem. C, 4 (2016) 8179-8188
- 106) P. Mishra, Sonia and P. Kumar J Alloy. Compd. 545 (2012) 210-215
- 107) Z.B. Pan, L.M. Yao, J.W. Zhai, B. Shen, S.H. Liu and H.T. Wang, etc J. Mater. Chem. A, 4 (2016) 13259-13264
- 108) S.H. Liu, J. Wang, B. Shen and J.W. Zhai J. Alloy. Compd. 696 (2016) 585-589
- 109) F. Fang, W.H. Yang, S.H. Yu, S.B. Luo and R.Sun, Appl. Phys. Lett. 104 (2014) 576
- 110) B. C. Keswani, S. I. Patil and Y. D. Kolekar AIP Conference Proceeding 1942 (2017) 140008-1-140008-4
- 111) P. S. Dobal, A. Dixit and R. S. Katiyar etc J. Appl. Phys. 89 (2001) 8085
- 112) W. Liu and X. Ren Phys. Rev. Lett. 103 (2009) 1
- 113) C. J. Xiao, C. Q. Jin and X. H. Wang Mater. Chem. Phys. 111 (2008) 209
- 114) C. A. Randallet al. J. Am. Ceram. Soc. 81 (1998) 677-88
- 115) W. Li, Z. Xu, R. Chu, P. Fu and G. Zang Phys. B. 405 (2010) 4513
- 116) R. Rani, S. Singh, J. K. Juneja and C. Prakash J. Integrated Ferroelectrics. 193:1 (2018) 66 – 71
- 117) Z. Xia and Q. Li Scripta Materials. 57 (2007) 981 – 984
- 118) D. Hennings, H. Schell and G. Simon J. Am. Ceram. Soc. 65 (1982) 539
- 119) A. Beauger, J. C. Mutin and J. C. Niepce J. Mater. Sci. 18 (1983) 3041
- 120) K. -i. Mimura, et al. Thin Solid Films. 516 (2008) 8408-8413
- 121) P.Victor, R. Ranjith and S. B. Krupanidhi J. Appl. Phys. 94 (2003) 7702-7709
- 122) M. Valant and D. Suvorov J. Am. Ceram. Soc. 87 (2004) 1222-1226
- 123) C. Ang, Z. jing and Z. Yu J. Phys. Condens. Matter. 14 (2002) 8901-8912
- 124) A. V. Tumarkin, M. V. Zlygostov and A. G. Gagartin J. Technical Physics Letters. 12 (2018) 1077 – 1080
- 125) C. Luo, J. Ji, F. Ling, D. Li and J. Yao J. Alloys. Compd. 687 (2016) 458
- 126) L. R. Song, Y. Chen, G. S. Wang and L. H. Yang etc J. Am. Ceram. Soc. 97 (2014) 3048
- 127) C. J. G. Meyers, C. R. Freeze, S. Stemmer, and R. A. York
- Appl. Surf. Sci. 424 (2017) 374

- 129) J. Zhang, X. Huang, S. Yu, and W. Zhang Ceram. Int. 42 (2016) 13262
- 130) H. N. Al-Shareef, K. D. Gifford, and S. H. Rou Integr. Ferroelectrics 3 (1993) 321
- 131) W. J. Jie, J. Zhu, W. F. Qin, X. H. Wei and J. Xiong, etc.J. Phys. D: Appl. Phys. 40 (2007) 2854
- 132) M. Wu, X. Li, S. Yu, Y. Sun, H. DongJ. Ceramics International. 45 (2019) 10917 10923
- 133) V. Lee, S. Lee, S. A. Sis and A. Mortazawi
  IEEE Trans. Microw.Theory Tech. 65 (2017) 3221-3229
- 134) Z. Yu, C. Ang, R. Guo and A. S. Bhalla Mater. Lett. 61 (2007) 326 – 329
- 135) R. Keech, C. Morandi, M. Wallace, L. Denisand and J. Guerrier etc J. Am. Ceram. Soc. 100 (2017) 3961 – 3972
- 136) M. Stengel and N. A. Spaldin Nature. 443 (2006) 679
- 137) C. S. HwangJ. Mater. Res. 16 (2001) 3476-3484
- 138) O. M. Hemeda, B. I. Salem, H. Abdelsatar, M. Shihab J.Physics B 574 (2019) 411680
- 139) N. Binhayeeniyi, P. Sukwisute, S. Nawae and N. Muensit J. Material 13 92020) 315
- 140) P. Sukwisute, N. Muensit, S. Soontaranon and S. Rugmai Appl. Phys.Lett. 103 (2013) 063905
- P. Rakbamrang, M. Lallart, D. Guyomar and N. MuensitSens. Actuators A Phys. 163 (2010) 493 500
- 142) N. Binhayeeniyi, P. Sukvisut, C. Thanachayanont and S. Muensit Mater. Lett. 64 (2010) 305–308
- 143) C. Thanachayanont, V. Yordsri, S. Kijamnajsuk and N. Binhayeeniyi *Mater. Lett.* 82 (2012) 205–207
- 144) H. Maiwa Ceram. Int.38 (2012) S219–S223
- 145) Q. Xu, D. Zhan, D. P. Huang and H. X. Liu etc. Mater. Res. Bull.47 (2012) 1674–1679
- 146) M. M. Ahmad, L. Alismail, A. Alshoaibi and A. Aljaafari etc.Results Phys. 15 (2019) 102799
- 147) M. TrainerJ. Phys. 21 (2000) 459–464
- 148) B. Liu, Y. Wu, Y. H. Huang, K. X. Song and Y. J. Wu J. Mater. Sci. 54 (2019) 4511–4517
- 149) Th. Wittinanon, R. Rianyoi, A. Chaipanich Journal of the European Ceramic Society 40 (2020)4886 – 4893
- 150) M. Nelo, T. Siponkoski, H. Kähäri, K. Kordas and J. Juuti etc. Journal of the European Ceramic Society 39 (2019) 3301-3306
- 151) R. Rianyoi, R. Potong, N. Jaitanong, R. Yimnirun and A. Chaipanich \ Applied Physics A: Materials Science and Processing 104(2) (2011) 661-666
- 152) R. Potong, R. Rianyoi, A. Ngamjarurojana, R. Yimnirun and R. Guo Ferroelectrics 455 (2013) 69-76
- 153) S. Huang, J. Chang, L. Lu, F. Liu, Z. Ye and X. Cheng Materials Research Bulletin 41 (2006) 291-297

- 154) S. Maji, P. Sarkar, L. Aggarwal, S.K. Ghosh and D. Mandal Physical Chemistry Chemical Physics 17 (2015) 8159-8165
- 155) G.B. Ghorbal, A. Tricoteaux, A. Thuault, G. Louis and D. Chicot Journal of the European Ceramic Society 37(6) (2017) 2531-2535
- 156) N. Nanakorn, P. Jalupoom, N. Vaneesorn and A. Thanaboonsombut, Ceramics International 34 (2008) 779-782
- 157) Z. Li, D. Zhang and K. Wu Journal of the American Ceramic Society 85 (2002) 305-313
- 158) M. Nelo, T. Siponkoski, H. Kähäri, K. Kordas, J. Juuti and H. Jantunen, Journal of the European Ceramic Society 39 (2019) 3301-3306
- 159) P. S. AktasJ. Chem. Sci. 132 (2020) 130
- 160) L. Dong, D. S. Stone and R. S. Lakes J. Appl. Phys. 111(2012) 084107
- 161) P. Seeharaj, B. Boonchom and P. Charoonsuk etc, Ceram. Int. 39 (2013) 559
- 162) J. Bera and S. K. RoutMater. Lett. 59 (2005) 135
- 163) I. Arvanitidis, D. Sichen and S. Seetharaman Mater. Trans. B Process Metall. Mater. Process. Sci. 27 (1996) 409
- 164) M. Sabet, M. Salavati-Niasari and Z. A. Fard Z A React. Inorganic Met. Nano-Metal Chem. 46 (2016) 317
- 165) M. M. Mikhailov, V. V. Neshchimenko, T. A. Utebekov and S. A. Yuriev J. Alloys Compd. 652 (2015) 364
- J. Q. Qi, Y. Wang, W. P. Chen, L. T. Li and H. L. W. ChanJ. Nanoparticle Res. 8 (2016) 959
- 167) T. Maiti, R. Guo and A. S. BhallaJ. Appl. Phys. 100 (2006) 114119
- 168) R. Chauhan and R. C. SrivastavaInt. J. Electron. Commun. Eng. 4 (2015) 1
- R. Varatharajana, S.B. Samantab and R. Jayavela, C. etc
   J. Materials Characterization 45 (2000) 89–93
- 170) Krishna PSR, Pandey D, Tiwari VS and Chakravarthy R Appl Phys.Lett 62 (1993)231–33
- 171) Xiaowen Z, Ying W and Longtu L.

  Journal of Ferroelectrics 101(1990) 61–74
- 172) Hamazaki SI, Shimizu F, Kojima S and Takashige M. J Phy Soc Jpn 64 (1995) 3660–63.

# 8 Graphical Abstract



## 9. Tables

Table 1: Coercive electric field  $(E_c)$ , remnant polarization  $(P_r)$ , maximum polarization  $(P_{max})$ , strain %,converse piezoelectric coefficient  $(d^*)$  values of BT, BCT8 and Fe doped BCT8

Composition	E <sub>C</sub> (kV/CM	P <sub>r</sub> (μC/CM	P <sub>max</sub> (μC/CM	Strain %(Pm/ V)			d*33 (pC/N)	
		,	,	-ve	+ve	-ve	+ve	
BT	2.53	6.38	20.43	0.133	0.137	335	339	
ВСТ	4.34	8.04	17.3	0.093	0.090	258	247	
BCT:1.25%Fe	4.88	0.99	10.8	0.077	0.077	101	98	
BCT:5%Fe	8.15	2.13	9.52	0.037	0.031	72	62	

Table 2: Dielectric constant  $(\epsilon')$  and dielectric loss  $(tan\delta)$ , Curie temperature  $(T_c)$ ,  $\epsilon'$  at  $T_c$  for BT, BCT and Fe-doped BCT

Composition	ε <sup>'</sup> @ RT	tanδ at RT	(T <sub>c</sub> ) °C	(ε') @ T <sub>c</sub>
BT	935	0.04	120	1691
BCT	980	0.025	135	4368
BCT:1.25%Fe	1234	0.020	Below RT	1275
BCT:5%Fe	1835	0.012	Below RT	1939

**Table 3**: Relative density, the values of the dielectric constant  $(\mathcal{E}_r)$  at  $T_m$  (1kHz), dielectric loss  $(\tan\delta)$  at  $T_m$  (1kHz), curie – Weiss temperature  $(T_0)$ , curie – Weiss law temperature  $(T_{cw})$ ,  $T_m$ ,  $\Delta T_m$ , and  $\gamma$  for all x values

$Ba(Zr_xTi_{1-x})O_3$	Relative Density (%)	$\varepsilon_{\mathbf{r}}$ at $T_m$ (1 kHz)	tanð at $T_m$ (1 kHz)	T <sub>0</sub> (K)	C (×10 <sup>5</sup> K)	<i>T<sub>cw</sub></i> ( <b>K</b> )	$T_m(\mathbf{K})$	$\Delta T_m$ ( <b>K</b> )	γ
X=0.00	93.26	9,496	0.0072	357	4.04	400	399	1	1.01
X=0.01	93.66	15,702	0.0207	366	4.08	395	392	3	1.05
X=0.03	93.76	19,698	0.0314	353	3.92	378	370	8	1.21
X=0.05	93.49	16,891	0.0382	335	3.79	368	353	14	1.26
X=0.08	93.32	11,294	0.0392	312	3.36	355	331	24	1.38

Table 4: Comparative study of various compositions and their different temperatures

Composition	Dopant	Calcination			Sintering			
		Temperature (°C)	Time (h)	Atmosphere	Temperature (°C)	Time (h)	Atmosphere	
Ba(Zr <sub>0.50</sub> Ti <sub>0.50</sub> )O <sub>3</sub>	Zr	100	24	Air	280	24	Air	
$\begin{array}{ccc} (Ba_{1-X}Ca_X) \\ (Ti_{0.9}Zr_{0.1})O_3 \ , & x \\ = 0.16 \end{array}$	Zr and Ca	1200	4	Air	1450	4	Air	
BaZr <sub>X</sub> Ti <sub>1-X</sub> O <sub>3</sub>	Zr	1670	2	Air	1750	4	Air	
$BaZr_{0.05}Ti_{0.95}O_{3}$	Zr	1200	2	Air	1400	2	Air	
Ba(Zr <sub>0.2</sub> Ti <sub>0.8</sub> )O <sub>3</sub> - 0.5(Ba <sub>0.7</sub> Ca <sub>0.3</sub> )TiO <sub>3</sub>	Zr and Ca	1	-		850	6	Air	
BZT/Mullite	Zr	1300	2	Air	1500	2	Air	
BZT/LSMO	Zr				900	2	Air	
Fe – doped Ca) TiO <sub>3</sub> (Ba –	Fe and Ca	1050	5	Air	1240	5	Air	
La-doped BZT	La and Zr	1473 K	4	Air	1673 K	6	Air	
$BaZr_{0.10}Ti_{0.90}O_3$	Zr	1100	4	Air	1350	4	Air	
$BaZr_{0.2}Ti_{0.8}O_3$	Zr	-	-		1250	8	Air	